Geochemical Evidence for a Comet Shower in the Late Eocene

K. A. Farley,* A. Montanari, E. M. Shoemaker,† C. S. Shoemaker

Analyses of pelagic limestones indicate that the flux of extraterrestrial helium-3 to Earth was increased for a 2.5-million year (My) period in the late Eocene. The enhancement began ~1 My before and ended ~1.5 My after the major impact events that produced the large Popigai and Chesapeake Bay craters ~36 million years ago. The correlation between increased concentrations of helium-3, a tracer of fine-grained interplanetary dust, and large impacts indicates that the abundance of Earth-crossing objects and dustiness in the inner solar system were simultaneously but only briefly enhanced. These observations provide evidence for a comet shower triggered by an impulsive perturbation of the Oort cloud.

The late Eocene is recognized as a period of elevated delivery of extraterrestrial matter to Earth. The 100-km-diameter Popigai crater and the 90-km-diameter Chesapeake Bay structure are the two largest known craters in the Cenozoic era and to within dating uncertainty occurred synchronously at 35.6 million years ago (Ma) (*1*, *2*). In addition to these and several smaller impact craters, at least two and possibly many more layers of impact debris including microspherules, Ir, and shocked quartz have been found in correlative sediments from around the world (3–6). Outside of this brief period, only a few additional impact layers are known from the entire geologic record. The explanation for this unusual episode is uncertain. Although it could be a statistical anomaly, it might also be the product of fast-path (*7*) delivery of asteroid fragments after collision in the asteroid belt or the result of a gravitational perturbation of the Oort cloud that enhanced the flux of new long-period comets—a comet shower (*8*). This ambiguity underscores our poor knowledge of the source of Earth-impacting bodies: The production of large impact craters may arise from temporally random delivery of asteroids and comets, from delivery of bursts of comets in brief showers, or from both (9). Theoretical considerations, chemical studies of impactites, and analyses of the terrestrial and planetary cratering records have been unable to resolve this issue. Here, we describe results of ^{3}He analyses of late Eocene sediments that provide a different approach to this problem.

Trace amounts of extraterrestrial matter can be detected in sea floor sediments with the use of the rare isotope of helium, ^{3}He. Compared with terrestrial matter, extraterrestrial matter is extremely enriched in this isotope, and one can use the distinction between terrestrial and extraterrestrial ^{3}He/^{4}He ratios ($<1 \times 10^{-7}$ versus $>1 \times 10^{-4}$, respectively) to unambiguously establish the fraction of sediment ^{3}He attributable to extraterrestrial sources. In many sediments, the extraterrestrial fraction approaches 100% of the ^{3}He in the sample (*10*, *11*). ^{3}He in the sedimentary record is sensitive only to the delivery of very fine-grained interplanetary dust particles (IDPs), because bodies larger than a few tens of micrometers in diameter are intensely heated and lose ^{3}He to the atmosphere and ultimately back to space (*12*). Thus, unlike platinum group metals, shocked quartz, and impact craters themselves, ^{3}He does not record the arrival of large objects. ^{3}He is a more sensitive tracer of IDPs than is Ir (*11*).

The extraterrestrial ^{3}He flux ranges as a function of the mass flux of IDPs and perhaps also as a consequence of changes in the intensity of the solar wind from which IDPs acquire He. An apparent correlation between periods of large impacts and enhanced ^{3}He flux in the Cenozoic era suggests that changes in the extraterrestrial mass flux are the dominant control (*12*). The present IDP flux is $\sim 40 \times 10^6$ kg year^{-1} (*13*) and is probably derived predominantly from asteroidal sources (*14*), although the mass flux and its sources must change over geologic time.

The concentration of extraterrestrial ^{3}He ($[^3\mathrm{He}]_{ET}$) in a sediment is governed by the relation $[^3\mathrm{He}]_{ET} = f_{3He}R/\alpha$, where f_{3He} is the flux of extraterrestrial ^{3}He, α is the sediment mass accumulation rate, and R is a postdeposition "retention" parameter varying between unity (quantitative retention) and zero (total loss). Recent work indicates that $^3\mathrm{He}_{ET}$ is retained for many hundreds of millions of years after deposition (*15*), mostly within or in intimate association with magnetite (*16*). Given such long-term retention, we assume that variations in R can be ignored over the relatively short period of interest for this work (the 4 My between 32 and 36 Ma).

Previous work on a North Pacific pelagic clay core has revealed a large and rapid increase in f_{3He} near the Eocene-Oligocene (E-O) boundary, but poor age control precludes precise correlation with known late Eocene impacts (*11*). The late Eocene to early Oligocene Massignano section in the Italian Apennines was selected for a detailed investigation of the relation between f_{3He} and major impacts through this interval. This well-documented sequence of pelagic limestones is the global stratotype and point for the E-O boundary (*17*). A 23-m exposure in an abandoned quarry, supplemented with a nearby drill core, provided samples from the period between ~36.5 and 31.6 Ma. Biostratigraphy, magnetostratigraphy, chemostratigraphy, and radiometric dates are available for these and related limestones of the Marche-Umbria Basin (*17*). Two <10-cm-wide layers of enhanced Ir occur at Massignano, at 5.61 and 10.25 m above the base of the exposed section (*5*). The 5.61-m anomaly is defined by four samples and has a maximum Ir concentration of about 200 parts per thousand (ppt). An impact origin is confirmed by the presence of shocked quartz in this interval (6). The 10.25-m Ir anomaly, although even larger than the first anomaly (330 ppt), was considered suspect because it was defined by just a single sample. Examination for shocked quartz has apparently never been undertaken on this interval.

Helium concentration and isotopic composition were measured on 79 Massignano limestone samples (*18*). Because the outcrop and core stratigraphy are carefully marked, we can relate our samples to previous measurements with <5-cm uncertainty. The mean sedimentation rate through the section is ~0.7 cm/thousand years (ky), so this uncertainty corresponds to <3 ky. ^{3}He/^{4}He ratios of 0.7 to 5×10^{-6} require the presence of extraterrestrial ^{3}He in the Massignano limestones (Fig. 1). Assuming reasonable He isotopic ratios for extraterrestrial (4×10^{-4}) and terrigenous (7×10^{-8}) components, the measured ^{3}He/^{4}He ratios indicate, that in most samples, $[^3\mathrm{He}]_{ET}$ is >80% of the total [^{3}He]. [^{3}He] ranges over an order of magnitude, from ~0.05 to ~0.6×10^{-12} cm^3 at standard temperature and pressure/g. Although there is substantial scatter in [^{3}He] over short vertical distances in the section, there is a

K. A. Farley, Division of Geological and Planetary Sciences, California Institute of Technology, MS 170-25, Pasadena, CA 91125, USA.
A. Montanari, Osservatorio Geologico di Coldigioco, 62020 Frontale di Apiro, Apiro, Italy, and Ecole des Mines de Paris, Paris, France.
E. M. Shoemaker and C. S. Shoemaker, U.S. Geological Survey, 2255 North Gemini Drive, Flagstaff, AZ 86001, USA.
*To whom correspondence should be addressed. E-mail: farley@gps.caltech.edu
†Deceased.

broad maximum between ~2 and ~15 m (Fig. 1A). $^3He/^4He$ variations show a similar distribution (Fig. 1B).

Extraterrestrial ^3He in a given sediment sample is hosted by a statistically small number of individual IDPs (*12*), leading to variability in measurements of [^3He] that likely contribute to the scatter in Fig. 1. To prevent this high-frequency noise from obscuring longer term trends, we drew a five-point running mean through the He data. The smoothed $[^3He]_{ET}$ retains the broad maximum between 2 and 15 m above the base of the section and has two peaks (defined by multiple analyses) at ~5 and 10 m. Throughout the uppermost part of the section (15 to 30 m), the smoothed $[^3He]_{ET}$ is nearly invariant, and the average through this younger interval is indistinguishable from the value below the broad maximum.

Although $[^3He]_{ET}$ is controlled by both f_{3He} and α, sedimentation rate changes are unlikely to be responsible for the variations in Fig. 1C. Paleomagnetism and radiometric ages suggest a relatively constant sedimentation rate through the Massignano section (*17*), yet the observed variations in $[^3He]_{ET}$ would require ~threefold slower sedimentation between 4 and 10 m than elsewhere in the section. Similarly, large changes in the sedimentation rate would almost certainly be accompanied by changes in the relative proportions of carbonate and noncarbonate matter. This expectation arises from the fact that the carbonate and noncarbonate components have different sources (biogenic versus mostly terrigenous matter). A decrease in the strength of one of these sources to produce a marked reduction in sediment mass accumulation rate would lead to an increase in the fraction of the other component in the sediment. The noncarbonate fraction is nearly invariant through the Massignano section, arguing against large mass accumulation rate changes (Fig. 1C). Perhaps most importantly, the position of the ^3He maximum is coincident with the previously reported impact indicators and with the ages of the Popigai and Chesapeake Bay impact structures.

Our data suggest an enhancement in f_{3He} over a 2.5-My period in the late Eocene, reaching ~5.5 times the nearly constant "baseline" value of the early Oligocene (Fig. 2). The enhancement begins before the first impact debris and craters at ~35.7 Ma. The maximum f_{3He} is coincident with the 5.61-m Ir anomaly, and although this peak appears to be a doublet, its structure may be an artifact of a sedimentation pulse associated with a prominent mica-bearing ash layer at 5.67 m (also evident from increased noncarbonate fraction; Fig. 1C). After this peak, f_{3He} declines for the next 1.7 My, except for a second peak, coincident with the 10.25-m Ir anomaly. The onset of this second f_{3He} peak again precedes the Ir anomaly, here by ~200 ky. Between 34.2 and 31.6 Ma, the flux is constant to ~±25% and has the same value as seen before ~36.3 Ma.

Although the maximum in $[^3He]_{ET}$ is temporally correlated with indicators of major impact events, the $[^3He]_{ET}$ enhancement is in comparison much longer lived (~15 m, 2.5 My), increasing before the appearance of impact debris and decreasing well after. The greater width of the ^3He peak relative to Ir cannot be attributed to bioturbation, because the length scale of bioturbation (~30 cm) is too small and in any case would broaden ^3He and Ir to a comparable extent. Nor can it result from diffusion, because once He is lost from its extraterrestrial host into intergranular voids, it will not be sampled by our technique. We conclude that f_{3He} began to increase more than half a million years before the Ir-producing impacts, reached maxima coincident with those impacts, and then declined over the next ~1 to 1.5 My.

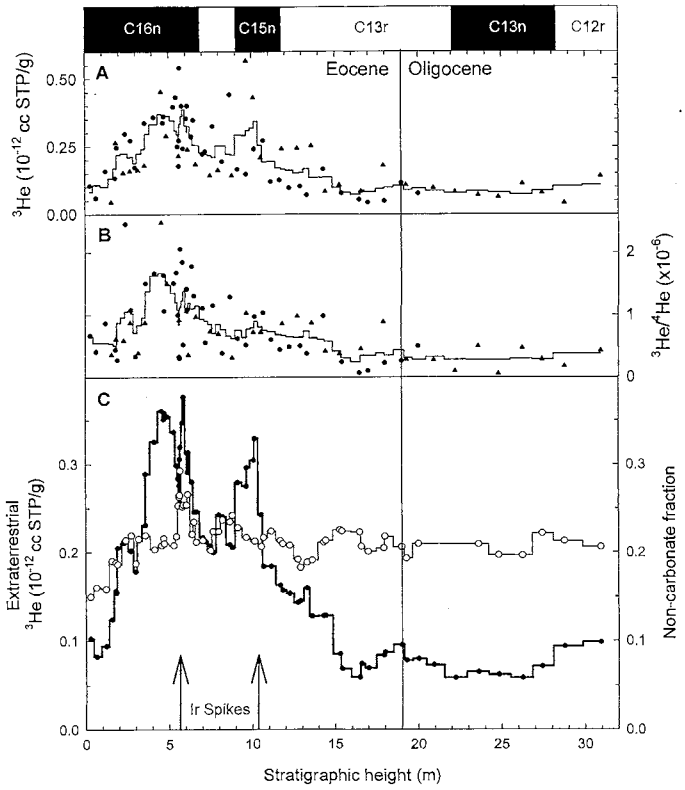

Fig. 1. Helium concentration and isotopic composition in the Massignano Quarry section (*17*) (●) and in the nearby Massicore drill core (*30*) (▲). (**A**) ^3He concentration. (**B**) $^3He/^4He$ ratios. (**C**) Extraterrestrial ^3He concentration (●, bold line) along with the measured fraction of noncarbonate material (○, light line). Stepped curves represent five-point running averages. In all three panels, the analytical uncertainties are comparable to the symbol size. Positions of Ir spikes (*5*), E-O boundary (*17*), and paleomagnetic reversal boundaries (top) (*30*) are indicated. Drill core samples were plotted at inferred stratigraphic position in the quarry section (*30*). cc STP/g, cubic centimeters at standard temperature and pressure per gram.

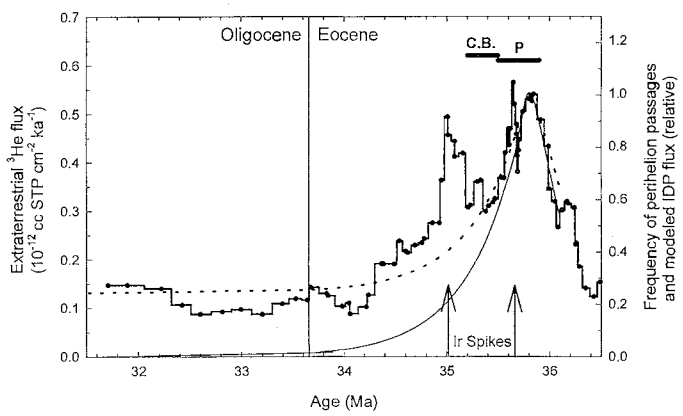

Fig. 2. Smoothed extraterrestrial ^3He flux (f_{3He}) and predictions for the IDP flux during a comet shower. f_{3He} (bold stepped curve) was computed from the extraterrestrial ^3He concentration (Fig. 1C), the mean sedimentation rate from Massignano chronostratigraphy (*5*, *30*), and a mean dry bulk density of 2.5 g cm^{-3}. The solid curve is the predicted frequency of perihelion passages during an impulsive comet shower (*8*), scaled to the height and centered on the position of the f_{3He} maximum. This curve is a reasonable measure of the enhancement in the cometary component of the IDP flux during a comet shower. The dotted curve is the same but is offset vertically and scaled to accommodate the preshower and postshower "baseline" IDP flux. The ages (±1σ) of the Popigai (P) and Chesapeake Bay (CB) impacts are indicated (*1*, *2*).

We consider two ways to produce the temporal relation between long-lived IDP flux enhancement and the occurrence of several major impacts in the late Eocene. The first involves a major collision or cratering event in the asteroid belt. Such a collision and the ensuing comminution of the resulting asteroid family could enhance the abundance of asteroidal dust. If the collision occurs sufficiently close to one of several known secular and mean-motion resonances, large bodies can be ejected from the asteroid belt to Earth-crossing orbits. Alternatively, large impactors and interplanetary dust may originate from cometary sources. Either mechanism can account for enhancement of the IDP flux at about the same time as major impacts occur on Earth.

A critical issue for evaluating these mechanisms is the time scale over which the IDP and large impactor flux evolve. Collisions can eject kilometer-class fragments from the asteroid belt that may achieve Earth-crossing orbits in <1 My (*7*) and may be removed from the solar system with a half-life of less than a few million years. Thus, asteroidal collisions may enhance the terrestrial impact probability for a few million years immediately after the collision and might be responsible for the impacts in the late Eocene. Interplanetary dust produced by the initial and ongoing collisions within the asteroid family will spiral into the sun under Poynting-Robertson drag and would be observed as an enhanced IDP flux at Earth within $\sim 10^4$ years of collision. Indeed, several asteroid families are associated with prominent dust bands that may dominate the current terrestrial IDP flux (*19*, *14*). We are not aware of any modeling of the evolution of the dust production rate after the initial formation of an asteroid family. However, modeling of the asteroid population in individual families indicates that they decay slowly, probably over many hundreds of millions of years; some of the asteroid families that have associated dust bands may be >100 My old (*20*). These observations suggest that the IDP production rate in an asteroid family may decay over a much longer time scale than the <2.5 My we observe in the late Eocene. In addition, an asteroidal collision event offers no obvious explanation for why the prominent peaks in IDP flux are closely correlated with impacts.

An alternative explanation is that the enhanced IDP flux and the impacts are associated with a comet or multiple comets. Comets are a source of particles in the zodiacal cloud (*21*), and because IDPs are swept into the sun on a time scale shorter than the average comet lifetime of 450 to 600 ky (*22*), the period of enhanced IDP flux should coincide with the most probable period of impacts. Typical long-period comets have a lifetime of ~600 ky, during which they make only ~five perihelion passages (*22*). Rather than the continuous and extended ^{3}He enhancement seen in the late Eocene, a single long-period comet would likely produce an increased ^{3}He flux over <1 My with pulses associated with each return. Similarly, the duration of activity of a single short-period comet (~100 ky) seems too short to account for the late Eocene enhancement. A more plausible explanation is a period of enhanced activity of long-period comets resulting from a gravitational perturbation of the Oort cloud, for example, caused by galactic tidal forces or a close encounter with a passing star (*23*, *24*). Small comet showers, capable of producing a few Earth impacts, are likely to occur on average every 30 to 50 My (*8*), although none have been conclusively demonstrated in the geologic record.

Modeling of the temporal evolution of an impulsive comet shower produced by a close stellar encounter shows that the frequency of comet perihelion passages (a measure of the likelihood of Earth impact) has an asymmetric shape, rising over a period of ~300 ky as comets arrive from the Oort cloud and then decaying with a half-period of ~600 ky (*8*). Assuming that the dust emission rate from these comets does not vary with time, the frequency of perihelion passages should be a reasonable measure of the cometary component of the terrestrial IDP flux. There is a strong similarity between this modeled frequency and the late Eocene enhancement of the ^{3}He flux (Fig. 2). The comet shower model predicts the duration and asymmetric shape of the $f_{^3He}$ profile, particularly when the early Oligocene "baseline" value (which probably originates in the asteroid belt) is added. Less obvious within this model is an explanation for the locally high $f_{^3He}$ values associated with the impacts recorded by Ir at 5.61 and probably 10.25 m. Although these short episodes may be attributed to cometary breakup events that briefly increase the IDP flux and the likelihood of Earth impact, it seems improbable that fragments of a single comet would dominate over the remainder of comets in the shower.

One potential difficulty with the comet shower model is that cometary IDPs, especially those derived from long-period comets, tend to travel on high-velocity orbits, which disfavors accretion to Earth and causes those particles that do accrete to be strongly heated and outgassed of ^{3}He during atmospheric entry. Nevertheless, some comets in a shower will have sufficiently low orbital inclination and eccentricity to permit entry at temperatures low enough to retain ^{3}He. In addition, orbital modeling indicates that interactions with Jupiter can slow down high-velocity cometary particles before terrestrial accretion (*25*).Thus, although it is not presently possible to scale the observed ^{3}He enhancement directly to an IDP mass flux increase, a correlation between the abundance of active comets and $f_{^3He}$ is reasonable.

Our preferred explanation for these data is that a short-lived burst of long-period comets occurred in the late Eocene. If this explanation is correct, then the Popigai and Chesapeake Bay impactors are likely to have been comets. This suggestion is consistent with the approximately chondritic elemental abundances inferred for the impactor component in the Popigai impact ejecta (*1*), although identification of the impactor by this technique is difficult (*26*), particularly in the case of Popigai, where the target lithologies are complex and poorly characterized (*27*). Additional evidence for a comet impact at this time comes from the recent discovery of abundant Ni-rich spinel, probably of cometary origin, associated with the 5.61-m Ir anomaly at Massignano (*28*).

Modeling suggests that a maximum in the cometary flux arising from tidal forces associated with the periodic motion of the solar system through the galactic disk should have occurred at nearly the same time as the Popigai and Chesapeake Bay impacts (*29*). Tidal forces are expected to enhance cometary activity over a protracted period, with a full width at half maximum of ~8 My (*29*). The enhancement is likely to be less than a factor of 4 in the total cometary flux and would likely rise and fall symmetrically. None of these predictions matches the late Eocene maximum. Thus, although the age of the proposed late Eocene comet shower is suggestive, our observations are more consistent with an isolated impulsive event than with a longer-duration periodic comet shower arising from galactic tidal forcing.

REFERENCES AND NOTES

1. R. Bottomley, R. Grieve, D. York, V. Masaitis, *Nature* **388**, 365 (1997).
2. C. Koeberl, C. W. Poag, W. U. Reimold, D. Brandt, *Science* **271**, 1263 (1996).
3. G. Keller, S. D'Hondt, T. L. Vallier, *ibid.* **221**, 150 (1983); J. Hazel, *Palaios* **4**, 318 (1988).
4. E. Molina, C. Gonzalvo, G. Keller, *Geol. Mag.* **130**, 483 (1993).
5. A. Montanari, F. Asaro, H. V. Michel, J. P. Kennett, *Palaios* **8**, 420 (1993).
6. A. Clymer, D. Bice, A. Montanari, *Geology* **24**, 483 (1996).
7. B. J. Gladman *et al.*, *Science* **277**, 197 (1997).
8. P. Hut *et al.*, *Nature* **329**, 119 (1987). Although the calculations of Hut *et al.* were for a major comet shower with a recurrence interval of ~400 My, the temporal evolution of smaller and more frequent showers will not be substantially different (P. Weissman, personal communication).
9. E. Shoemaker, R. Wolfe, C. Shoemaker, in *Global Catastrophes in Earth History*, V. Sharpton and P. Ward, Eds. (Geological Society of America, Boulder, CO, 1990), pp. 155–170.
10. C. Merrihue, *Ann. N.Y. Acad. Sci.* **119**, 351 (1964); M. Ozima, M. Takayanagi, S. Zashu, S. Amari, *Nature* **311**, 449 (1984).

11. K. A. Farley, *Nature* **376**, 153 (1995).
12. ———, S. G. Love, D. B. Patterson, *Geochim. Cosmochim. Acta* **61**, 2309 (1997).
13. S. G. Love and D. E. Brownlee, *Science* **262**, 550 (1993).
14. S. Dermott *et al.*, in *Physics, Chemistry and Dynamics of Interplanetary Dust*, B. Gustafson and M. Hanner, Eds. (Astronomical Society of the Pacific, San Francisco, CA, 1996), vol. 104, pp. 143–153.
15. D. B. Patterson, K. A. Farley, B. Schmitz, in preparation.
16. S. Amari and M. Ozima, *Nature* **317**, 520 (1985).
17. I. Premoli-Silva, R. Coccioni, A. Montanari, Eds., *The Eocene-Oligocene Boundary in the Marche-Umbria Basin (Italy)* (International Union of Geological Sciences, Ancona, Italy, 1988).
18. Limestone samples of ~2.5 g were dried at 90°C overnight, powdered, sieved, and dissolved in 10% acetic acid. After complete decarbonation, the residue was isolated, dried, weighed (to obtain the noncarbonate fraction), and transferred to a tinfoil packet. The packet was fused in vacuum, and the evolved He was purified and analyzed by mass spectrometry (*11*). The estimated analytical uncertainty on [^{3}He] and ^{3}He/^{4}He determinations is <3%. We report [^{3}He] per gram of bulk limestone. In some cases, replicate analyses were made; the mean value is plotted.
19. S. Dermott, P. Nicholson, J. Burns, J. Houck, *Nature* **312**, 505 (1984).
20. F. Marzari, D. Davis, V. Vanzani, *Icarus* **113**, 168 (1995).
21. J. C. Liou, S. F. Dermott, Y. L. Xu, *Planet. Space Sci.* **43**, 717 (1995).
22. P. Weissman, *Nature* **344**, 825 (1990).
23. J. Hills, *Astron. J.* **86**, 1730 (1981); P. Weissman, *Earth Moon Planets* **72**, 25 (1996).
24. M. Rampino and R. Stothers, *Nature* **308**, 709 (1984).
25. J. Liou and H. Zook, *Icarus* **123**, 491 (1996).
26. R. Grieve and L. Pesonen, *Earth Moon Planets* **72**, 357 (1996).
27. S. A. Vishnevsky and A. Montanari, in preparation.
28. O. Pierrard, E. Robin, R. Rocchia, A. Montanari, *Geology* **26**, 307 (1998).
29. J. J. Matese, P. G. Whitman, K. A. Innanen, M. J. Valtonen, *Icarus* **116**, 255 (1995).
30. L. Lanci, W. Lowrie, A. Montanari, *Earth Planet. Sci. Lett.* **143**, 37 (1996).
31. We thank P. Weissman for a constructive and thoughtful review and D. Patterson and K. Robinson for assistance with sample preparation. Supported by NASA and by the David and Lucille Packard Foundation through a fellowship award to K.A.F.

13 January 1998; accepted 27 March 1998

Fullerene Pipes

Jie Liu, Andrew G. Rinzler, Hongjie Dai, Jason H. Hafner, R. Kelley Bradley, Peter J. Boul, Adrian Lu, Terry Iverson, Konstantin Shelimov, Chad B. Huffman, Fernando Rodriguez-Macias, Young-Seok Shon, T. Randall Lee, Daniel T. Colbert, Richard E. Smalley*

Single-wall fullerene nanotubes were converted from nearly endless, highly tangled ropes into short, open-ended pipes that behave as individual macromolecules. Raw nanotube material was purified in large batches, and the ropes were cut into 100- to 300-nanometer lengths. The resulting pieces formed a stable colloidal suspension in water with the help of surfactants. These suspensions permit a variety of manipulations, such as sorting by length, derivatization, and tethering to gold surfaces.

Single-wall carbon nanotubes (SWNTs) of molecular perfection—fullerene nanotubes—are of great interest because of their unique electronic (*1*) mechanical (*2*) properties combined with chemical stability. The present availability of various fullerene structures reveals a large gap in the intermediate size range between small spheroidal fullerenes and long SWNTs. This intermediate size range could, however, be of paramount scientific and technological importance. For example, fullerene tubes in the length range of 10 to 300 nm might provide connectors and components for molecular electronic devices. We report here methods that make available, in substantial quantities, fullerene macromolecules occupying this intermediate length range. Our approach involves cutting the nearly endless, highly tangled ropes of nanotubes that are currently available (*3*, *4*) into short lengths of open tubes—fullerene pipes—so they can be suspended, sorted, and manipulated as individual macromolecules.

A vital step in developing the molecular science and technology of these fullerene macromolecules is to take advantage of the rich chemistry available at their ends. We also report here the rational derivatization of these fullerene pipes. The ongoing elaboration of these structures should result in a class of organic molecules with the potential for broad applications.

The SWNTs for this study were prepared by a scaled-up version (*5*) of the laser-oven method described previously (*3*, *6*). Although this method produces fullerene nanotube material of lower quality (50%) than the previously described method (70 to 90%), it has the advantage of being able to produce 20 g of material in 2 days of continuous operation. This as-grown material contains a substantial fraction of nanoscale impurities (bucky onions, spheroidal fullerenes, amorphous carbon, and others) that are difficult to separate from the nanotubes once they have been cut. For this reason, it became imperative that the starting material be purified before cutting. Previously reported purification methods for multiwalled carbon nanotubes (MWNTs) (*7*) and SWNTs (*8*) either totally destroy or are ineffective at purifying the present SWNT material in large amounts. Ultimately, we developed a purification method that consists of refluxing in 2.6 M nitric acid and resuspending the nanotubes in pH 10 water with surfactant followed by filtration with a cross-flow filtration system (*9*).

Passing the resultant purified SWNT suspension through a polytetrafluoroethylene filter produced a free-standing mat of tangled SWNT ropes—a "bucky paper." Typical scanning electron microscope (SEM) images near and at a torn edge of a paper are shown in Fig. 1, B and C, respectively. As is evident in Fig. 1C, the tearing process produces a substantial alignment of the SWNT ropes. The net yield of purified fullerene fibers from this method depends on the initial quality of the raw material, with typical yields in the range of 10 to 20% by weight. A particularly low-quality starting material (Fig. 1A) was chosen to highlight the efficacy of the method. Survival of such a high percentage of these fibers after refluxing for days in nitric acid is indicative of the high degree of molecular perfection of their sidewalls.

Extensive SEM and transmission electron microscope imaging of the fullerene rope fibers in these purified samples shows them to be highly tangled with one another and so long that their ends are rarely visible. The frequent occurrence of fullerene toroids ("crop circles") in these samples (*10*) suggests that fullerene rope ends are hard to find because many of the ropes are, in fact, truly endless. We suspect that this condition results from van der Waals adherence of the "live" ends of the ropes to the sides of other ropes as growth proceeds in the argon atmosphere of the laser-oven method. The growing rope ends are then eliminated in collisions with other live rope ends growing along the same guiding rope from the opposite direction. In one dimension, collisions are unavoidable.

We verified that one can cut and make ends from these tangled, nearly endless ropes by several techniques ranging from simply cutting with a pair of scissors to

J. Liu, A. G. Rinzler, H. Dai, J. H. Hafner, R. K. Bradley, P. J. Boul, A. Lu, T. Iverson, K. Shelimov, C. B. Huffman, F. Rodriguez-Macias, D. T. Colbert, R. E. Smalley, Center for Nanoscale Science and Technology, Rice Quantum Institute, Departments of Chemistry and Physics, Rice University, Houston, TX 77005, USA.
Y.-S. Shon and T. R. Lee, Department of Chemistry, University of Houston, Houston, TX 77204, USA.

*To whom correspondence should be addressed. E-mail: res@cnst.rice.edu